

Theory of Electron Spin Relaxation in ZnO

N.J. Harmon,¹ W.O. Putikka,¹ and R. Joynt²

¹*Physics Department, Ohio State University, 191 W. Woodruff Ave., Columbus, OH 43210, USA*

²*Physics Department, University of Wisconsin-Madison, 1150 University Ave., WI 53705, USA*

(Dated: October 24, 2018)

Doped ZnO is a promising material for spintronics applications. For such applications, it is important to understand the spin dynamics and particularly the spin relaxation times of this II-VI semiconductor. The spin relaxation time τ_s has been measured by optical orientation experiments, and it shows a surprising non-monotonic behavior with temperature. We explain this behavior by invoking spin exchange between localized and extended states. Interestingly, the effects of spin-orbit coupling are by no means negligible, in spite of the relatively small valence band splitting. This is due to the wurtzite crystal structure of ZnO. Detailed analysis allows us to characterize the impurity binding energies and densities, showing that optical orientation experiments can be used as a characterization tool for semiconductor samples.

I. INTRODUCTION

Zinc Oxide has been the subject of considerable experimental and theoretical investigation for many years.¹ Its bandgap is in the near ultraviolet, making it useful as a transparent conductor and as sunscreen. Its piezoelectricity opens up transduction applications. The activity has intensified more recently because of the possibility that ZnO might be useful for spintronics or spin-based quantum computation. It has been predicted to be a room-temperature ferromagnet when doped with Mn.² Furthermore, its spin-orbit coupling is generally thought to be very weak compared with GaAs. The usual measure of the strength of spin-orbit coupling in semiconductors is the energy splitting at the top of the valence band. It is said that the spin-orbit coupling is negligible in ZnO because the valence-band splitting is -3.5 meV,³ as opposed to 340 meV for GaAs. Smaller spin-orbit coupling should lead to long spin relaxation times. Long relaxation times are required if spin information is to be transported over appreciable distances.

The spin relaxation time τ_s has been measured by Ghosh et al.⁴ to be about 20 ns from 0 to 20 K in optical orientation experiments. τ_s is sometimes called T_2^* even in the absence of an external field. Since the data from Ref. (4) used in this paper were taken at zero field, the relaxation time is taken to be τ_s to avoid confusion with experiments conducted at finite field. The data show two surprising features. First, the relaxation times are actually somewhat shorter than the longest relaxation times in GaAs, which are about 100 ns.⁵ One might expect the opposite given the relative strength of spin-orbit coupling in the two materials. Second, τ_s shows a non-monotonic temperature dependence, first increasing slightly and then rapidly decreasing - but increasing temperature usually promotes spin relaxation.

In this paper, we show that a theory previously developed for τ_s in GaAs⁶ can account for these observations. The theory must be modified to take account of the different impurity levels and binding energies of ZnO. This is important, because, in spite of intensive investigation, the nature of the impurities that govern the electrical properties of ZnO remains controversial, and our analysis sheds some light on this issue. Even more interestingly, it turns out that the wurtzite crystal

structure has very important consequences for the D'yakonov-Perel (DP)⁷ scattering that dominates the relaxation at higher temperatures. Thus the crystal structure must be taken into account fully. The final message will be that the "weak" spin-orbit coupling of ZnO is not negligible for spin relaxation, and it does not lead to long relaxation times.

In the next section we give the background information for ZnO. Sec. III is devoted to a derivation of the equations of motion for the spins. In Sec. IV the computational method is described. The determination of the parameters in the equations of motion is a separate task. The most important of the parameters is that which controls that DP spin relaxation. Since the calculation of this parameters is not straightforward, we devote Sec. V to that. Sec. VI gives the results. Sec. VII is the conclusions and puts the results into context.

II. BACKGROUND

In ZnO produced by the hydrothermal method, it is generally thought that there are two sets of impurity states, one shallow and quasi-hydrogenic, one deep and very well localized.^{8,9} Their precise physical nature is not known. In the case of the deep impurity, it is believed that a lattice defect accompanies the chemical impurity. The binding energies are in the range of a few 10s of meV for the shallow impurity and a few 100s of meV for the deep impurity. We shall demonstrate below that the optical orientation data can put bounds on these numbers.

ZnO crystallizes in the wurtzite structure rather than the zincblende structure familiar from the III-V compounds. This has very important implications for the conduction band states. The spin-orbit interaction lifts the spin degeneracy in the conduction band. In zincblende structures crystal symmetry implies that the splitting is cubic in the magnitude of the wavevector k , but in the wurtzite structure the splitting is linear.¹⁰ However, the spin relaxation time of the low-lying conduction band states depends mainly on the spin splitting near the conduction band minimum, and this is larger in ZnO than in GaAs for small enough k .

In optical orientation experiments, electrons are excited from the valence band to the conduction band by circularly

polarized light tuned close to the bandgap energy (pump step). The population of conduction electrons so created is spin-polarized.¹¹ Energy relaxation then occurs on a short time scale (≤ 1 ns), but most of this relaxation is from spin-conserving processes, so there is a longer time scale (or time scales) on which the spin of the system relaxes. When an external magnetic field is present, the time scale to relax the transverse component of the *net* magnetization is called τ_s . It is measured using Faraday rotation or the Kerr effect (probe step).

The important physical point is that the fast energy relaxation leads to a thermal charge distribution for the electrons by the time 1 ns has elapsed, but the spin distribution relaxes on longer time scales. The thermal charge distribution means that the localized donor impurity states are mostly full at the relatively low temperatures of the experiment. The spins of the localized electrons must be included along with the conduction electron spins. The spins of localized and extended states can be interchanged by the exchange coupling, a process we call cross-relaxation. This is often a rather fast process and is particularly important when the relaxation times of the localized and extended states are very different in magnitude. In GaAs this process is important in all the regimes of temperature, applied field, and impurity density that have been studied, and it is important in ZnO as well.

In the following section we derive a set of modified Bloch equations to describe the aforementioned spin dynamics.

III. MODIFIED BLOCH EQUATIONS

We consider a conduction electron in the semiclassical approximation. It moves as a wavepacket with a well-defined momentum and scatters from impurities and phonons at time intervals of average length τ_p , where τ_p is the momentum relaxation time. Its spin operator is \mathbf{s}_c . The spin-dependent part of its Hamiltonian in the absence of an external magnetic field is:

$$H^c = H_1^c + H_2^c = -\frac{1}{2\hbar} \sum_i J(\mathbf{r} - \mathbf{R}_i) \mathbf{s}_i \cdot \mathbf{s}_c - g \frac{\mu_B}{\hbar} \mathbf{b}(t) \cdot \mathbf{s}_c. \quad (1)$$

The first term, H_1^c , is the exchange interaction with impurity spins \mathbf{s}_i located at an positions \mathbf{R}_i . It is the same interaction that is responsible for the Kondo effect, but the temperatures here are all much greater than the Kondo temperature. The range of the function $J(\mathbf{r} - \mathbf{R}_i)$ is roughly a_B , where a_B is the effective Bohr radius. The second term, H_2^c , represents other spin relaxation mechanisms that we model as a small random classical field $\mathbf{b}(t)$ with a correlation time much shorter than τ_s . An analogous Hamiltonian H^l can be written for a localized electron.

First, we concentrate on the spin dynamics resulting from the spin-spin term and ignore the second term. In the dilute limit ($a_B n_{imp}^{1/3} \ll 1$), a conduction electron encounters impurities with randomly aligned spins if no short-range order is present in the impurity system. An effective field from the impurity spin affects the conduction electron when it is within

$\sim a_B$ of the impurity. When $|\mathbf{r} - \mathbf{R}_i| > a_B$, the conduction electron proceeds unhindered by the effective field. This effective field is a result of the exchange potential. An itinerant electron will spend an average time of a_B/v within the range of the effective field where v is the velocity of the electron. Thus the time between encounters¹² is $1/n_I a_B^2 v$.

In a semiclassical picture the spin of the itinerant electron undergoes precession of magnitude $\Delta\phi = Ja_B/2v$ through a random angle during each encounter with an impurity. The spin of the impurity electron also precesses but with angle $-\Delta\phi$. Since the sum of spins, $\mathbf{s}_c + \mathbf{s}_l$, commutes with $H_1^c + H_1^l$, the total spin in the system must be conserved. However the spin in each subsystem may shift between one another; this is cross-relaxation.

It turns out for the parameters of the system under consideration that $\Delta\phi \sim 1$, and we then find that

$$\tau_c^{cr} \sim \frac{1}{n_I a_B^2 v} \quad (2)$$

which implies that the spin is essentially randomized after one impurity encounter.

If we consider an ensemble of conduction electrons with a net magnetization m_c , this magnetization is exchanged at a rate of $1/\tau_c^{cr}$. As previously mentioned, any magnetization lost from the conduction electrons must be gained by the localized electrons and vice-versa. For clarity we write $1/\tau_c^{cr} = n_I/\gamma^{cr}$ and $1/\tau_l^{cr} = n_c/\gamma^{cr}$ where $\gamma^{cr} = 1/a_B^2 v$.

We now examine the second term of the Hamiltonian

$$H_2^c(t) = -\frac{1}{2} g \mu_B (b_x(t) \sigma_x + b_y(t) \sigma_y + b_z(t) \sigma_z). \quad (3)$$

This Hamiltonian relaxes the conduction electron spin. To extract a relaxation rate from this Hamiltonian, we use the equation of motion

$$\frac{d\rho(t)}{dt} = \frac{i}{\hbar} [\rho(t), H_2^c(t)] \quad (4)$$

where $\rho(t)$ is the 2×2 spin density matrix for an electron of a given momentum. We assume that the total density matrix for the conduction electron factorizes; we neglect off-diagonal terms that come from correlations. By iteration, we can write this equation as

$$\left\langle \frac{d\rho(t)}{dt} \right\rangle = \frac{i}{\hbar} \langle [\rho(0), H_2^c(t')] \rangle - \frac{1}{\hbar^2} \int_0^t \langle [[\rho(t'), H_2^c(t')], H_2^c(t)] \rangle dt' \quad (5)$$

where the angular brackets indicate averaging over all orientations of $b(t)$. To simplify notation, from now on angular brackets will be suppressed on the density matrix. Since $\langle b_i(t) \rangle = 0$, the first term is zero. We assume that different directions of b_i are uncorrelated and (since the external field is zero) different direction are equivalent. Then we have $\langle b_i(t) b_j(t') \rangle = \langle b(t) b(t') \rangle \delta_{i,j}$. Therefore, Eq. (5) reduces to

$$\frac{d\rho(t)}{dt} = -\frac{g^2 \mu_B^2}{2\hbar^2} \int_0^t \sum_i [\rho(t'), \sigma_i] \sigma_i \langle b(t) b(t') \rangle dt'. \quad (6)$$

The correlation function is assumed to be stationary in time so $\langle b(t)b(t') \rangle = g(t' - t) = g(\tau)$.¹³ If the correlation time of the b -fluctuations, τ_e , is short, ρ will not change on that timescale and $g(\tau)$ will be nearly a δ -function (Markov approximation). Eq. (6) can then be written as

$$\frac{d\rho(t)}{dt} = -\frac{2g^2\mu_B^2}{\hbar^2} \frac{1}{4} \sum_i [\rho(t), \sigma_i] \sigma_i \int_0^\infty \langle b(t)b(t') \rangle dt'. \quad (7)$$

The integral is approximated by $\langle b^2 \rangle \tau_e$. Define the relaxation time scale τ_c by

$$\frac{1}{\tau_c} = 2 \left(\frac{g\mu_B}{\hbar} \right)^2 \langle b^2 \rangle \tau_e \quad (8)$$

giving

$$\frac{d\rho(t)}{dt} = -\frac{1}{4\tau_c} \sum_i [\rho(t), \sigma_i] \sigma_i. \quad (9)$$

The density matrix can be expanded in Pauli spin matrices

$$\rho(t) = \frac{1}{2} I + \frac{1}{2} \sum_i m_i(t) \sigma_i. \quad (10)$$

where I is the 2×2 identity matrix and $m_i = \text{Tr}(\sigma_i \rho)$ is the expected value of the magnetization. Inserting Eq. (10) in Eq. (9) and matching coefficients of Pauli matrices gives a set of equations for the dynamics of \mathbf{m} . For instance for conduction electron magnetization m_c in the x -direction, $dm_c/dt = \text{Tr}(\sigma_x d\rho/dt) = -m_c/\tau_c$. As with H_1^c , similar expressions for the localized magnetization m_l can be found: $dm_l/dt = \text{Tr}(\sigma_x d\rho/dt) = -m_l/\tau_l$.

By combining the effects of $H_1 = H_1^c + H_1^l$ and $H_2 = H_2^c + H_2^l$, the modified Bloch equations for the magnetizations can be expressed as

$$\begin{aligned} \frac{dm_c}{dt} &= -\left(\frac{1}{\tau_c} + \frac{n_l}{\gamma^{cr}} \right) m_c + \frac{n_c}{\gamma^{cr}} m_l \\ \frac{dm_l}{dt} &= \frac{n_l}{\gamma^{cr}} m_c - \left(\frac{1}{\tau_l} + \frac{n_c}{\gamma^{cr}} \right) m_l. \end{aligned} \quad (11)$$

for two spin systems - itinerant and localized spins. τ_c and τ_l in Eq. (11) are now described in terms of well known relaxation mechanisms which will be discussed in the next section. This model was successfully applied to GaAs.⁶ For ZnO, these Bloch equations are easily extended to account for the multiple-type impurities present.

IV. METHOD

We now seek to write equations like those of Eq. (11) with regard given to the two types of impurities in ZnO - shallow and deep. As mentioned above, we find that the cross-relaxation is important to understand the data. These rates come from the Kondo-like $J\mathbf{s}_l \cdot \mathbf{s}_c$ interaction between an impurity spin \mathbf{s}_l and a conduction band spin \mathbf{s}_c . An expression for J in terms of tight-binding parameters can be derived using the Schrieffer-Wolf transformation.¹⁴ One expects that

the cross-relaxation between conduction and shallow donor electrons to be much more rapid than the cross-relaxation between conduction and deep donor electrons because of the greater binding energy of the deep impurity and its larger on-site Coulomb energy. This is confirmed by the fit to the data. In fact we find that terms involving cross-relaxation between the deep donors and either the conduction band electrons or the shallow donor electrons can be neglected. With these simplifications, for ZnO Eq. (11) extends to

$$\begin{aligned} \frac{dm_c}{dt} &= -\left(\frac{1}{\tau_c} + \frac{n_{ls}}{\gamma_{c,s}^{cr}} \right) m_c + \frac{n_c}{\gamma_{c,s}^{cr}} m_{ls} \\ \frac{dm_{ls}}{dt} &= \frac{n_{ls}}{\gamma_{c,s}^{cr}} m_c - \left(\frac{1}{\tau_{ls}} + \frac{n_c}{\gamma_{c,s}^{cr}} \right) m_{ls} \\ \frac{dm_{ld}}{dt} &= -\frac{1}{\tau_{ld}} m_{ld}. \end{aligned} \quad (12)$$

In this equation, m_c , m_{ls} , and m_{ld} stand for the magnetizations of the conduction electrons, the electrons on shallow impurities, and the electrons on deep impurities, respectively. The n 's denote the corresponding volume densities. Each of the populations has a relaxation time τ_c , τ_{ls} , and τ_{ld} . From Eq. (12), we can then find the magnetization as a function of time.

Standard methods can be used to solve these differential equations. The solutions yield a time dependence of the total magnetization, $m(t) = m_c(t) + m_{ls}(t) + m_{ld}(t)$, to be a sum of three exponentials, $\exp(-\Gamma_+ t)$, $\exp(-\Gamma_- t)$, and $\exp(-\Gamma_d t)$ where

$$\Gamma_\pm = \frac{1}{2} \left(\frac{1}{\tau_c} + \frac{1}{\tau_{ls}} + \frac{n_c + n_{ls}}{\gamma_{c,s}^{cr}} \pm S \right), \quad \Gamma_d = \frac{1}{\tau_{ld}} \quad (13)$$

with S given by

$$S = \sqrt{\left(\frac{1}{\tau_{ls}} - \frac{1}{\tau_c} + \frac{n_c - n_{ls}}{\gamma_{c,s}^{cr}} \right)^2 + \frac{4n_c n_{ls}}{\gamma_{c,s}^{cr 2}}}. \quad (14)$$

No net moment can exist on the deep donor sites since no moment is excited into the deep states on account of them being significantly below the conduction band, and no net moment cross relaxes into these states. Therefore Γ_d can be ruled out as being the observed relaxation rate. In the regime that $(n_{ls} + n_c)/\gamma_{c,s}^{cr} \gg 1/\tau_c$, $1/\tau_{ls}$, the rate Γ_+ simplifies to $(n_c + n_{ls})/\gamma_{c,s}^{cr}$ and is very rapid and the rate Γ_- is slower,

$$\Gamma_- = \frac{n_c}{n_c + n_{ls}} \frac{1}{\tau_c} + \frac{n_{ls}}{n_c + n_{ls}} \frac{1}{\tau_{ls}}. \quad (15)$$

We fit the data with this equation and associate it with τ_s . We see that the relaxation rate depends on two factors: the thermodynamic occupations of the shallow donors (the deep donors are always nearly full in the temperature range studied here) and form of the relaxation rates for the conduction and localized shallow states.

The densities can be computed using standard formulas from equilibrium statistical mechanics, since we deal only with time scales long compared to the fast energy relaxation

scale. As a function of temperature T , the ratio n_c/n_{ls} naturally increases rapidly as $T \rightarrow |\epsilon_{ls}|/k_B$, where ϵ_{ls} is the binding energy of the shallow impurity. $|\epsilon_{ld}|$ is so large that these states are always occupied at the experimental temperatures, which range from 5K to 80K.

τ_c is fairly complicated to calculate because there are several mechanisms that can relax the conduction electron spins. The simplest such mechanism is the Elliot-Yafet (EY) process¹⁵ that arises from spin mixing in the wavefunctions. When a conduction electron is scattered by a spin-independent potential from state \mathbf{k} to state \mathbf{k}' , the initial and final states are not eigenstates of the spin projection operator S_z so the process relaxes the spin. The rate of relaxation due to the EY process is well known to be of the form: $1/\tau_{EY} = \alpha_{EY}T^2/\tau_p(T)$ where α_{EY} is a material dependent parameter and τ_p is the momentum relaxation time.¹⁶ We estimate $\alpha_{EY}(th) = 4.6 \times 10^{-15} \text{ K}^{-2}$. The Bir-Aronov-Pikus (BAP) mechanism¹⁷ arises from the scattering of electron and holes. This relaxation mechanism is commonly considered to be negligible in n -type materials like those under consideration here since the number of holes is small.¹⁸ The D'yakonov-Perel' (DP) mechanism⁷ arises from the ordinary scattering of conduction-band states. Since this has not previously been calculated in a wurtzite structure, we devote the next section to it. This calculation yields an expression for τ_c as a function of temperature.

τ_{ls} and τ_{ld} are due to non-spin-conserving anisotropic exchange (Dzyaloshinski-Moriya) interactions.^{19,20} The anisotropic exchange term is important. It arises from spin-orbit coupling and produces a term proportional to $\mathbf{d} \cdot \mathbf{s}_1 \times \mathbf{s}_2$ where \mathbf{d} is related to the interspin separation and the exchange integral between the wavefunction on sites 1 and 2. However, it is not possible to calculate it in detail when the nature of the impurities is not well known. We estimate the rate as $1/\tau_{DM} = \alpha_{DM}(n_{imp,s} + n_{imp,d})$ where $n_{imp,s}$ and $n_{imp,d}$ are the total impurity concentrations of the shallow and deep impurity respectively and α_{DM} has a weak temperature dependence that we neglect. The main contribution comes from the the overlap of the shallow impurity wavefunctions, which we take to be hydrogenic, with the deep impurity wavefunctions, which we take to be well-localized on an atomic scale. The details of how to estimate the resulting relaxation may be found in Refs. (6,21,22). The numerical value we find from theory is $\alpha_{DM}(th) = 1.12 \times 10^{-20} \text{ cm}^3 \text{ ns}^{-1}$. When nuclei possess nonzero magnetic moments, the hyperfine interaction between electron and nuclear spin is a source of spin relaxation for localized electrons.²³ However, zero nuclear spin isotopes of Zn and O are 96% and 99.5% naturally abundant respectively. Therefore we rule out the hyperfine interaction from being an observed relaxation mechanism in Ref. (4).

V. DP MECHANISM IN WURTZITE CRYSTAL STRUCTURES

The conduction band states undergo ordinary impurity and phonon scattering. Each scattering event give a change in the

wavevector \mathbf{k} , which in turn changes the effective magnetic field on the spin that comes from spin-orbit coupling. This fluctuating field relaxes the spin. The effective field strength is proportional to the conduction band spin splitting. Bulk zincblende crystals have conduction band splittings cubic-in- k due to bulk inversion asymmetry (Dresselhaus effect).²⁴ In addition to cubic terms, bulk wurtzite conduction bands also possess spin splittings proportional to linear terms in k due to the hexagonal c axis which gives bulk wurtzite a reflection asymmetry similar to the Rashba effect.^{10,25,26,27} We can write the spin-orbit Hamiltonian to include both the Rashba and Dresselhaus terms:

$$H_{so}(\mathbf{k}) = [\alpha\kappa_1 + \gamma\kappa_3] \cdot \sigma \quad (16)$$

where $\kappa_1 = (k_y, -k_x, 0)$ is linear-in- k , $\kappa_3 = (k_{||}^2 - bk_z^2)(k_y, -k_x, 0)$ is cubic-in- k , $\sigma = (\sigma_x, \sigma_y, \sigma_z)$ are the Pauli spin matrices, and α, γ are spin splitting coefficients.^{10,26,28} The parameter b is roughly equal to four for all wurtzite materials.²⁸ Note that there is no spin splitting along the hexagonal axis (z).

The linear-in- k term dominates and we can determine the spin relaxation rate by following the treatment given by Pikus and Titkov in Ref. (29) which yields the following relaxation rates:

$$\frac{1}{\tau_{DP,ii}^{(1)}} = \tilde{\tau}_p \frac{4\alpha^2}{\hbar^2} (\overline{\kappa_1^2} - \overline{\kappa_{1,i}^2}) \quad (17)$$

$$\frac{1}{\tau_{DP,i \neq j}^{(1)}} = \tilde{\tau}_p \frac{4\alpha^2}{\hbar^2} \overline{\kappa_{1,i}\kappa_{1,j}} \quad (18)$$

where the overbar denotes angular averaging, and i, j denote the Cartesian components of κ_1 . The momentum relaxation rate is defined as

$$\frac{1}{\tilde{\tau}_p} = \int_{-1}^1 \sigma(\theta)(1 - \cos\theta)d\cos\theta \quad (19)$$

where $\sigma(\theta)$ is the scattering cross section and θ is the angle between initial and final \mathbf{k} .²⁹ In bulk wurtzite $\overline{\kappa_{1,||}^2} = \overline{\kappa_{1,x}^2} = \overline{\kappa_{1,y}^2} = k^2/3$, $\overline{\kappa_{1,z}^2} = 0$, and in the unstrained crystal, $\overline{\kappa_{1,i}\kappa_{1,j}} = 0$ for $i \neq j$. From Eq. (17), we can write

$$\frac{1}{\tau_{DP,||}^{(1)}} = \frac{2}{\tau_{DP,z}^{(1)}} = \frac{4}{3} \frac{\alpha^2}{\hbar^2} \tilde{\tau}_p k^2 = \frac{8}{3} \frac{m^* \alpha^2}{\hbar^4} \tilde{\tau}_p E_{\mathbf{k}} \quad (20)$$

where m^* is the electron effective mass and $E_{\mathbf{k}}$ is the energy $\hbar^2 k^2 / 2m^*$. This result can be Boltzmann averaged (denoted by angle brackets) to obtain

$$\frac{1}{\tau_{DP}^{(1)}(T)} = \left\langle \frac{1}{\tau_{DP,||}^{(1)}} \right\rangle = \frac{8}{3} \frac{m^* \alpha^2}{\hbar^4} \langle \tilde{\tau}_p E_{\mathbf{k}} \rangle = \alpha_{DP}^{(1)} \tau_p(T) T \quad (21)$$

where $\alpha_{DP}^{(1)} = 4m^* \alpha^2 k_B / \hbar^4$ and $\tau_p(T) = \langle \tilde{\tau}_p E_{\mathbf{k}} \rangle / \langle E_{\mathbf{k}} \rangle = 2 \langle \tilde{\tau}_p E_{\mathbf{k}} \rangle / 3k_B T$. The temperature dependent momentum relaxation time, $\tau_p(T)$, can be determined from electron mobility (μ_e) measurements from $\mu_e = e\tau_p(T)/m^*$ where e is the

charge of an electron. α has been calculated¹⁰ to be 1.1×10^{-4} eV-nm which gives a theoretical value of $\alpha_{DP}^{(1)}(th) = 34.6 \text{ K}^{-1} \text{ ns}^{-2}$.

Similarly, the cubic-in- k term can be calculated to be

$$\frac{1}{\tau_{DP}^{(3)}(T)} = \frac{1}{\tau_{DP,\parallel}^{(3)}(T)} = \frac{2}{\tau_{DP,z}^{(3)}(T)} = \alpha_{DP}^{(3)} \tau_p(T) T^3 \quad (22)$$

where $\alpha_{DP}^{(3)} = 80Q\gamma^2 m^* k_B^3 / 3\hbar^8$ where the dimensionless quantity Q depends on the type of scattering and is of order unity. γ has been calculated¹⁰ to be 3.3×10^{-4} eV-nm³ which yields $\alpha_{DP}^{(3)}(th) = 2.0 \times 10^{-4} \text{ K}^{-3} \text{ ns}^{-2}$.

The sample from which the momentum relaxation times $\tau_p(T)$ were extracted³⁰ was hydrothermally grown by the same company as Ghosh et al. sample in Ref. (4).

VI. RESULTS AND DISCUSSION

In Fig.1 we show that temperature dependence of τ_s as measured in a bulk ZnO sample and our fit (using Eq. (15)) to the data. It is seen immediately that the temperature dependence is not monotonic and that this is well-reproduced by the theory. The reason is simple. At low temperatures $T \ll |\epsilon_{ls}|/k_B$ nearly all the electrons are in localized states. These states relax by the temperature-independent DM mechanism: $1/\tau_s = 1/\tau_{DM}$. This mechanism alone determines the $T = 0$ values. When T approaches $|\epsilon_{ls}|/k_B$, the deep impurities are all occupied but the rest of the population is shared by shallow localized and conduction band states. Initially, the conduction band electrons have a longer spin lifetime because impurity scattering is frequent at low temperatures so the DP mechanism that relaxes them is not very effective. However, the DP mechanism increases rapidly as T increases and the τ_s curve turns around. At $T \gg |\epsilon_{ls}|/k_B$, the shallow impurity level is empty and the relaxation is dominated by the DP mechanism in the conduction band: $1/\tau_s = 1/\tau_{DP}^{(1)}(T)$.

At this point it is necessary to point out why only the linear-in- T DP mechanism is needed to explain the observed conduction spin relaxation. The other two viable candidates (cubic DP and EY) for relaxation are much too weak to explain the observed relaxation times in ZnO. We use the calculated values for $\alpha_{DP}^{(1)}(th)$ and $\alpha_{DP}^{(3)}(th)$ in the previous section to obtain the relative relaxation efficiencies between the linear and cubic DP mechanism terms:

$$\frac{1/\tau_{DP}^{(1)}}{1/\tau_{DP}^{(3)}} = \frac{\alpha_{DP}^{(1)}(th)}{\alpha_{DP}^{(3)}(th)T^2} = \frac{1.73 \times 10^5 \text{ K}^2}{T^2} \quad (23)$$

which demonstrates that the efficiency of the cubic-in- T term does not become comparable to the linear-in- T term at temperatures below 416 K which is far above the temperature range investigated here. In fact the cubic-in- T term does not even reach one-tenth the efficiency of the linear-in- T term in the temperature range investigated here. For this reason we can confidently ignore the cubic-in- T DP mechanism term in our fit. The crystal structure of ZnO therefore makes its spin

relaxation qualitatively different from spin relaxation in bulk n -GaAs. We also compare the efficiencies of the DP and EY mechanisms:

$$\frac{1/\tau_{DP}^{(1)}}{1/\tau_{EY}} = \frac{\alpha_{DP}^{(1)}(th)\tau_p^2(T)}{\alpha_{EY}(th)T} = \frac{7.5 \times 10^{15}\tau_p^2(T) \text{ K ns}^{-2}}{T}. \quad (24)$$

Even if the momentum relaxation time taken to be unrealistically low, say 1 fs, the DP mechanism is still nearly two orders of magnitude more efficient at relaxing spins than the EY mechanism in the temperature range studied here. Due to the drastic qualitative and quantitative differences between relaxation mechanisms, we have unequivocally determined the relevant conduction electron spin relaxation mechanism in ZnO.

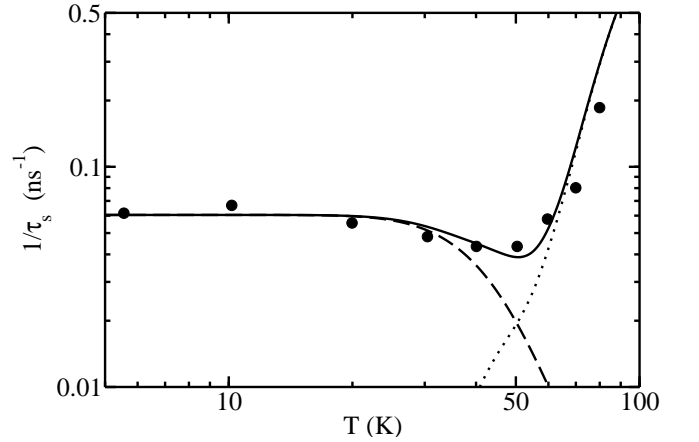


FIG. 1: Plot of $1/\tau_s$ vs. temperature. Points are experiment of Ref. 4. Dashed curve: $[n_{ls}/(n_c + n_{ls})](1/\tau_{DM})$. Dotted curve: $[n_c/(n_c + n_{ls})](1/\tau_{DP})$. Solid curve: total $1/\tau_s$. $n_{imp,s} = 6.0 \times 10^{14} \text{ cm}^{-3}$, $n_{imp,d} = 5.0 \times 10^{17} \text{ cm}^{-3}$, $\epsilon_{ls} = -23 \text{ meV}$, and $\epsilon_{ld} = -360 \text{ meV}$.

The fit of theory to the experimental data is clearly very good. We found that no reasonable fit was possible using only a single impurity level, though this worked very well for GaAs⁶, so we used two levels. A good fit by this method was possible by adjusting the coefficients $\alpha_{DP}^{(1)}(exp)$ and $\alpha_{DM}(exp)$, and the binding energies $\epsilon_{ls}, \epsilon_{ld}$ and concentrations $n_{imp,s}, n_{imp,d}$ of the two donors, subject to the constraint that the room temperature carrier density should equal the measured⁴ value of $1.26 \times 10^{15} \text{ cm}^{-3}$. Qualitatively, one finds that $n_{imp,d} \gg n_{imp,s}$ and $|\epsilon_{ld}| \gg |\epsilon_{ls}|$ to get the right order of magnitude of the relaxation at low T . Physically, the deep impurity spins are important because they relax the shallow impurity spins by the DM mechanism, and the strength of the low T relaxation implies that the deep impurities must be quite numerous. Quantitatively, a least squares fit to the data of Ref. (4) yields $\alpha_{DP}^{(1)}(exp) = 134.5 \text{ K}^{-1} \text{ ns}^{-2}$, $\alpha_{DM}(exp)n_{imp,d} = 0.06 \text{ ns}^{-1}$, $|\epsilon_{ld}| = 360 \text{ meV}$, $|\epsilon_{ls}| = 23 \text{ meV}$, and $n_{imp,s} = 6.0 \times 10^{14} \text{ cm}^{-3}$.

$\alpha_{DP}^{(1)}(exp)$ is about four times larger than the theoretical value of $\alpha_{DP}^{(1)}(th)$ given above, possibly due to strain effects. We also note that the values of τ_p that we used were taken from a different sample.

If we take $n_{imp,d}$ to be near the highest values measured for the deep donor (see below) then $\alpha_{DM}(exp) = 12 \times 10^{-20} \text{ cm}^3 \text{ ns}^{-1}$ is about one order of magnitude larger than the theoretical estimate $\alpha_{DM}(th)$ given above. In view of the very poor understanding of the impurity wavefunctions, and the exponential dependence of α_{DM} on the overlaps, this is perhaps not too disturbing.

The presence of a shallow donor and a very deep donor has been seen in hydrothermally grown ZnO samples of the type investigated here.^{9,31} Donor concentrations up to nearly $5.0 \times 10^{17} \text{ cm}^{-3}$ ($n_{imp,d}$) have been measured for donors 330 – 360 meV ($|\epsilon_{d|}$) deep.^{9,31,32} Donors as shallow as 13 – 51 meV ($|\epsilon_{s|}$) have been measured⁸ at lower concentrations $\sim 5.0 \times 10^{14} \text{ cm}^{-3}$ ($n_{imp,s}$). Comparison with our values indicates that the parameters extracted from the fit are very reasonable for this material.

From this analysis, we predict that in ZnO samples with fewer deep impurities, the relaxation time at low temperatures can be increased. As the impurities of ZnO vary greatly between different growth techniques³³, this prediction could be tested by further optical orientation experiments on different samples.

VII. CONCLUSIONS

We have found that τ_s in bulk ZnO can be understood by invoking previously known spin relaxation mechanisms. The dominant mechanisms in the material turn out to be the DP (scattering) relaxation of the conduction electron spins for $T > 50 \text{ K}$ and the DM (anisotropic exchange) mechanism for the localized spins for $T < 50 \text{ K}$. In addition, it is very impor-

tant to include the cross-relaxation between localized and conduction states previously proposed for GaAs. These physical ingredients explain quantitatively the relatively fast relaxation at low temperatures as being due mainly to the DM mechanism which in turn depends on having both deep and shallow impurity states. At high temperatures, the conduction states are dominant, and the DP mechanism gives an excellent fit to the data. The combination explains the very surprising non-monotonic temperature dependence of τ_s .

Finally, there are two aspects of the data in Ref. (4) that we have not addressed here: the applied magnetic field dependences on the spin relaxation and the spin relaxation observed in ZnO epilayers. We plan on addressing the former issue in a future publication. As for the latter issue, the epilayers are doped three to four orders of magnitude higher than in the bulk case. At such high dopings, spin glass effects become important and localized donor states coalesce to produce donor bands; we do not expect our theory to be applicable in such a regime.

The theory has now been sufficiently developed that optical orientation experiments can actually serve as a characterization tool for doped semiconductors, giving information about the binding energies and concentrations of the electrically active impurities in n -type materials.

We would like to acknowledge useful discussions with S. Ghosh. Financial support was provided by the National Science Foundation, Grant Nos. NSF-ECS-0523918 (NH and WP) and NSF-ECS-0524253 (RJ).

-
- ¹ Ü. Özgür, Ya. I. Alivov, C. Liu, A. Teke, M. A. Reshchikov, S. Doğan, V. Avrutin, S. J. Cho, and H. Morkoç, *J. Appl. Phys.* **98**, 041301 (2005).
 - ² T. Dietl, H. Ohno, F. Matsukura, J. Cibert, and D. Ferrand, *Science* **287**, 1019 (2000).
 - ³ W. J. Fan, J. B. Xia, P. A. Agus, S. T. Tan, S. F. Yu, and X. W. Sun, *J. Appl. Phys.* **99**, 013702 (2006).
 - ⁴ S. Ghosh, V. Sih, W. H. Lau, and D. D. Awschalom, *Appl. Phys. Lett.* **86**, 232507 (2005).
 - ⁵ J. M. Kikkawa and D. D. Awschalom, *Phys. Rev. Lett.* **80**, 4313 (1998).
 - ⁶ W. O. Putikka and R. Joynt, *Phys. Rev. B* **70**, 113201 (2004).
 - ⁷ M. I. Dyakonov and V. I. Perel, *Sov. Phys. JETP* **33**, 1053 (1974).
 - ⁸ H. von Wenckstern, H. Schmidt, M. Grundmann, M. W. Allen, P. Miller, R. J. Reeves, and S. M. Durbin, *Appl. Phys. Lett.* **91**, 022913 (2007).
 - ⁹ U. Grossner, S. Gabrielsen, T. M. Børseth, J. Grillenberger, A. Y. Kuznetsov, and B. G. Svensson, *Appl. Phys. Lett.* **85**, 2259 (2004).
 - ¹⁰ L. C. Lew Yan Voon, M. Willatzen, M. Cardona, and N. E. Christensen, *Phys. Rev. B* **53**, 10703 (1996).
 - ¹¹ M. I. Dyakonov and V. I. Perel, in *Optical Orientation*, edited by F. Meier and B. P. Zacharenya (North-Holland, Amsterdam, 1984).
 - ¹² K. Seeger, *Semiconductor Physics*, 6th ed. (Springer, New York, 1997), p. 161.
 - ¹³ C. P. Slichter, *Principles of Magnetic Resonance*, 3rd ed. (Springer, New York, 1990), pp. 192, 207.
 - ¹⁴ J. R. Schrieffer and P. A. Wolff, *Phys. Rev.* **149**, 491 (1966).
 - ¹⁵ R. J. Elliott, *Phys. Rev.* **96**, 266 (1954).
 - ¹⁶ J. N. Chazalviel, *Phys. Rev. B* **11**, 1555 (1975).
 - ¹⁷ G. L. Bir, A. G. Aronov, and G. E. Pikus, *Sov. Phys. JETP* **42**, 705 (1976).
 - ¹⁸ Pil Hun Song and K.W. Kim, *Phys. Rev. B* **66**, 035207 (2002).
 - ¹⁹ I. Dzyaloshinskii, *Phys. Chem. Solids* **4**, 241 (1958).
 - ²⁰ T. Moriya, *Phys. Rev.* **100**, 91 (1960).
 - ²¹ L. P. Gor'kov and P. L. Krotkov, *Phys. Rev. B* **67**, 033203 (2003).
 - ²² K. V. Kavokin, *Phys. Rev. B* **69**, 075302 (2004).
 - ²³ I. Zutic, J. Fabian and S. Das Sarma, *Rev. Mod. Phys.* **76**, 323 (2004).
 - ²⁴ G. Dresselhaus, *Phys. Rev.* **100**, 580 (1955).
 - ²⁵ E. I. Rashba, *Sov. Phys. Solid State* **2**, 1109 (1960).
 - ²⁶ J. Y. Fu and M. W. Wu, arXiv:0805.1577v2 (2008).
 - ²⁷ W. Weber, S. D. Ganichev, S. N. Danilov, D. Weiss, and W. Prettl, *Appl. Phys. Lett.* **87**, 262106 (2005).
 - ²⁸ W.-T. Wang, C. L. Wu, S. F. Tsay, M. H. Gau, Ikai Lo, and H. F. Kao, *Appl. Phys. Lett.* **91**, 082110 (2007).
 - ²⁹ G. E. Pikus and A. M. Titkov, in *Optical Orientation*, edited by

- F. Meier and B. P. Zachachrenya (North-Holland, Amsterdam, 1984).
- ³⁰ D. C. Look, *Surface Science* **601**, 5315 (2007).
- ³¹ C. H. Seager and S. M. Myers, *J. Appl. Phys.* **94**, 2888 (2003).
- ³² G. H. Kassier, M. Hayes, and F. D. Auret, *J. Appl. Phys.* **102**, 014903 (2007).
- ³³ D. C. Look, *Materials Science and Engineering B* **80**, 383 (2001).